

# Diffusion Monte Carlo evaluation of disiloxane linearisation barrier

Adie Tri Hanindriyo<sup>1,\*</sup>, Amit Kumar Singh Yadav<sup>2,†</sup>, Tom Ichibha<sup>3,†</sup>, Ryo Maezono<sup>4,†</sup>, Kousuke Nakano<sup>4,5,†</sup> and Kenta Hongo<sup>6†</sup>

<sup>†1</sup> *School of Materials Science, JAIST, Asahidai 1-1, Nomi, Ishikawa, 923-1292, Japan*

<sup>‡2</sup> *Department of Electrical Engineering, Indian Institute of Technology Gandhinagar, Palaj 382355, Gujarat, India*

<sup>¶3</sup> *Materials Science and Technology Division, Oak Ridge National Laboratory, Oak Ridge, Tennessee 37831, USA*

<sup>§4</sup> *School of Information Science, JAIST, Asahidai 1-1, Nomi, Ishikawa, 923-1292, Japan*

<sup>||5</sup> *Scuola Internazionale Superiore di Studi Avanzati(SISSA), via Bonomea, 265-34136 Trieste ITALY.*

<sup>⊥6</sup> *Research Center for Advanced Computing Infrastructure, JAIST, Asahidai 1-1, Nomi, Ishikawa 923-1292, Japan*

E-mail: adietri@icloud.com

## Abstract

The disiloxane molecule is a prime example of silicate compounds containing the Si-O-Si bridge. The molecule is of significant interest within the field of quantum chemistry, owing to the difficulty in theoretically predicting its properties. Herein, the linearisation barrier of disiloxane is investigated using a fixed-node diffusion Monte Carlo (FNDMC) approach, which is currently the most reliable *ab initio* method in accounting for an electronic correlation. Calculations utilizing the density functional theory (DFT) and the coupled cluster method with single and double substitutions, including noniterative triples (CCSD(T)) are carried out alongside FNDMC for comparison. Two families of basis sets are used to investigate the disiloxane linearisation barrier - Dunning's correlation-consistent basis sets cc-pV $x$ Z ( $x = D, T, \text{ and } Q$ ) and their core-valence correlated counterparts, cc-pCV $x$ Z. It is concluded that FNDMC successfully predicts the disiloxane linearisation barrier and does not depend on the completeness of the basis sets as much as DFT or CCSD(T), thus establishing its suitability.

## INTRODUCTION

The simplest molecule containing the Si-O-Si bond is disiloxane or Si<sub>2</sub>H<sub>6</sub>O. Also called disilyl ether, its structure is a single Si-O-Si bond terminated by three H atoms at each end (H<sub>3</sub>Si-O-SiH<sub>3</sub>). There have been numerous studies investigating the Si-O-Si bond, particularly owing to its importance in the modelling of silica compounds, which are the most abundant constituent of the Earth's crust. Most importantly, silica compounds range in function from glasses to quartz crystals, both of which comprise large sectors in industry. In some studies, disiloxane has been used as a sealant and as a component in cosmetics, or as a prototype region of a zeolite or clay substrate for applications ranging from catalysis to prebiotic synthesis.<sup>1</sup>

Experimental evaluations of the Si-O-Si bond indicate an anharmonic bending potential with a low linearisation barrier, which makes it quite difficult to attain sufficient accuracy in such measurements.<sup>2,3</sup> Despite the significant volume of previous studies dedicated to the Si-O-Si bond,<sup>1,4-10</sup> the properties of Si-O-Si bond obtained in most of these studies are not consistent with each other. In

*ab initio* studies, in particular, multiple calculation methods have resulted in different values for the bond angle and length,<sup>9,11,12</sup> as well as the linearisation energy<sup>4,5,8</sup> and Si-O-Si potential energy surface,<sup>1,9</sup> among other factors. These properties and the bond geometry itself are shown to be sensitive to the choice of basis set and level of theory (the former more than the latter) according to at least one previous study.<sup>8</sup>

To narrow down the possibilities, it would be ideal to employ the most reliable methods at our disposal. Quantum Monte Carlo (QMC), currently the most reliable of the many-body calculation methods, is expected to provide a reasonable and reliable prediction.<sup>13</sup> We used the fixed-node diffusion Monte Carlo (FNDMC) method, which has been widely and successfully applied to several molecular systems.<sup>14–21</sup> Although FNDMC results are also affected by the choice of basis sets,<sup>18,22</sup> we note that the basis-set dependence is considerably different from that for an SCF-based method, such as the density functional theory (DFT) and molecular orbital (MO) methods. In SCF-based approaches, the choice of basis set affects both the amplitude and the nodal positions of the corresponding many-body wavefunctions (although the methods do not explicitly employ a many-body wavefunction condition). With FNDMC, by contrast, the choice only affects the nodal positions. The amplitude can be automatically adjusted such that its shape may approach that of the exact solution as closely as possible under a restriction with a fixed nodal position.<sup>13,23</sup> A typical example is the description of electron-nucleus cusps.<sup>24</sup> Even when using such a poor basis set that cannot describe the singularity of the cusp based on its analytical form, an initial guess is applied for further numerical evolution driven by the FNDMC, making the amplitude at the nucleus positions singular with a cusp.<sup>13,23</sup> Owing to this self-healing property of the amplitude, the dependence on the choice of basis sets in FNDMC becomes considerably weaker. That is, the bias arising from the choice is reduced more than that for SCF-based ones, which is a difficulty faced by the present systems.<sup>8</sup> Note that “cusplless” basis sets cause a singularity of the local energy in FNDMC, thus resulting in numerical instability. However, this sin-

gularity can be easily remedied by introducing the cusp correction proposed by Ma et al.<sup>24</sup>

In this study, we applied FNDMC to investigate the basis-set dependence of the linearisation energy of a disiloxane molecule in comparison with other *ab initio* methods including DFT and CCSD(T), as well as empirical measurements from earlier studies conducted on disiloxane.<sup>2,3,25</sup> The FNDMC depends on the basis set implicitly through its fixed nodal surface provided by the Slater determinant whose orbitals are expanded in terms of the basis set, whereas DFT and CCSD(T) strongly depend on the choice of basis set. The cc-pVxZ<sup>26–28</sup> and cc-pCVxZ<sup>29</sup> basis sets ( $x = D, T, Q$ ), which are standard correlation methods, were examined in the present study and then applied to all the *ab initio* calculations to investigate the basis-set dependence of linearisation energy evaluation.

## MODEL AND METHODOLOGY

Our target property is simply a linearisation barrier of disiloxane  $\text{Si}_2\text{H}_6\text{O}$  between “linear” and “non-linear” (bent) structures. As can be seen from Figure 1, the linear structure possesses an eclipsed  $D_{3h}$  symmetry<sup>7</sup> and a non-linear structure is a bent conformation of the  $C_{2v}$  symmetry.<sup>30</sup> For the two fixed structures, the barrier,  $\Delta E_{\text{barrier}}$ , is defined as the energy difference between the linear and non-linear structures:

$$\Delta E_{\text{barrier}} = E_{\text{linear}} - E_{\text{delinear}}, \quad (1)$$

where  $E_{\text{linear}}$  and  $E_{\text{delinear}}$  are the (electronic) total energies of the linear and non-linear structures, respectively.

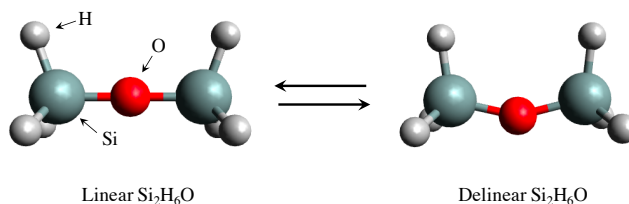


Figure 1: Linear and non-linear molecular structures of disiloxane,  $\text{Si}_2\text{H}_6\text{O}$ .

The accuracy of computed  $\Delta E_{\text{barrier}}$  values can be calibrated by referring to experimentally observed  $\Delta E_{\text{barrier}}$  values. To compare our computational results with the experimental results, however, we note that the experimental  $\Delta E_{\text{barrier}}$  involves the zero-point energy (ZPE) contribution, whereas our computational  $\Delta E_{\text{barrier}}$  value considers only the electronic contribution. The ZPE contributions can also be evaluated at each level of theory, although their accuracy depends on methods adopted and the basis sets. To investigate the basis-set dependence of  $\Delta E_{\text{barrier}}$ , we simply consider the electronic  $\Delta E_{\text{barrier}}$ . Thus, the experimental  $\Delta E_{\text{barrier}}$  values are corrected by adopting a theoretical estimate from Koput.<sup>6</sup> We address this issue in more detail later.

In the present study, the above two energies  $E_{\text{linear}}$  and  $E_{\text{delinear}}$  were computed through various combinations of (1) *ab initio* methods and (2) basis sets

(1) Our methods applied are DFT with B3LYP exchange-correlation functional<sup>31</sup> (DFT-B3LYP), CCSD(T),<sup>32</sup> and FNDMC<sup>13</sup> with trial wavefunctions generated from DFT-B3LYP. Within the framework of DFT, DFT-B3LYP is a standard method for covalent systems. Within the correlated methods, CCSD(T) is known to be the ‘‘gold standard’’ in quantum chemistry. A variety of methods and basis sets were chosen in line with the previous results<sup>8</sup> indicating dependence of the Si-O-Si bond description on such choice. FNDMC is known to be comparable with CCSD(T); however, for the first time, we applied FNDMC to an evaluation of  $\Delta E_{\text{barrier}}$ .

(2) Our basis sets are a family of Dunning’s correlation-consistent basis sets (cc-pV $x$ Z;  $x = \text{D, T, Q}$ )<sup>26–28</sup> and their core-valence correlated variants (cc-pCV $x$ Z;  $x = \text{D, T, Q}$ ).<sup>29</sup> The cc-pV $x$ Z and cc-pCV $x$ Z basis sets were originally developed for correlated methods such as CCSD(T), but have been found to be appropriate even for DFT-B3LYP and FNDMC in properly reproducing the dynamic electron correlation.<sup>26</sup> In particular, the polarisation functions included implicitly in cc-pV $x$ Z are essential for properly describing the Si-O-Si bond. To describe the correlation effects more precisely, the present study considers the dynamic correlation between core and va-

lence electrons by applying the cc-pCV $x$ Z basis sets, which can reproduce the core-valence correlation by minimising the difference in the correlation energies between all-electron and valence-only (using pseudopotentials) calculations.<sup>33</sup> The number of basis functions entailed in each basis set is shown in Table 1. As shown, accounting for the core-valence correlation is more expensive for increasingly complete orbital and polarisation functions, with a quadruple zeta-level basis set adding close to 130 more basis functions to the standard correlation-consistent basis set. The number of basis functions is expected to largely correlate with the reliability of the calculations, particularly for the core-valence variants pertaining to all-electron calculations.

**Table 1: List of basis functions**

Basis set	Linear basis functions
cc-pVDZ	80
cc-pCVDZ	102
cc-pVTZ	182
cc-pCVTZ	245
cc-pVQZ	353
cc-pCVQZ	482

In the present study we obtained the linear and delinear structures using the second-order Møller-Plesset perturbation theory (MP2) with the cc-pVQZ basis set (MP2/cc-pVQZ level), and previous studies conducted at the MP2/cc-pVQZ level of theory<sup>7,11</sup> have established a reliable favourability toward a delinear structure and provide good agreement for the Si-O-Si angle in accordance with experimental results.<sup>30</sup> Modelling of the Si-O-Si angle in particular has been heavily emphasised in previous theoretical studies for both disiloxane<sup>8</sup> and pyrosilic acid.<sup>9,10</sup> This necessitates even larger numbers of basis functions, which means that the cc-pCVQZ basis set would necessitate the highest number of basis functions by far. The two optimised structures at the MP2/cc-pVQZ level of theory were used in this work to calculate all  $\Delta E_{\text{barrier}}$  values, i.e., common to all levels of theory, where the linear structure has a Si-O-Si angle of 180° and the delinear structure has an optimised Si-O-Si angle of 146.8° comparable with the experimental value of 144.1°.<sup>30</sup> The other

structural parameters are given in the Supporting Information, and are also in good agreement with experiments.

The present study adopted no pseudopotential calculations, but rather all-electron calculations with a total of 42 electrons for a single disiloxane molecule. This molecular system is not so large that the CCSD(T) calculation within the frozen core approximation is feasible, despite the computational cost of CCSD(T) scaling as  $N^7$ , where  $N$  is the number of electrons in the system. By contrast, the DFT cost scales with  $N^3$  (or less) and is therefore unimportant. Similar to DFT, the FNDMC cost scales as  $N^3$ , although the prefactor of FNDMC is much larger than that of DFT. This is because a vast number of random sampling points are required to obtain a sufficiently small error bar (sub-chemical accuracy of  $\sim 0.1$  kcal/mol) to calibrate a small  $\Delta E_{\text{barrier}}$  ( $\sim 0.5$  kcal/mol). Recent parallel computers, however, enable us to apply FNDMC to evaluate such a tiny  $\Delta E_{\text{barrier}}$ , because its algorithm is intrinsically parallel.

In our FNDMC calculations, we adopted Slater-Jastrow type wavefunctions as their fixed-node trial wavefunctions.<sup>34</sup> Molecular orbitals entering the single Slater determinants were generated by DFT-B3LYP with various types of basis sets. The Jastrow factor consists of one-, two-, and three-body terms<sup>35</sup> including 88 variational parameters in total. These parameters were optimised through a variance minimisation scheme,<sup>36</sup> and only the two-body term holds the electron-electron cusp condition.<sup>37</sup> The electron-nucleus cusp condition, which is a short-range one-body correlation effect, is satisfied by the cusp correction scheme applied to the Gaussian basis sets<sup>24</sup> instead of imposing the cusp condition on the one-body term. Note that the Jastrow factor does not change the (fixed) nodal surfaces and is responsible for the numerical stability in FNDMC. However, the quality of the nodal surfaces determines the accuracy of the FNDMC energies in terms of the fixed-node variational principles.<sup>38</sup> Accordingly, the FNDMC accuracy depends implicitly on the basis set adopted, which is used to expand the molecular orbitals entering the Slater determinant. In addition to the fixed-node error, another source of bias in actual FNDMC calculations arises from the short-time

approximation with finite (small) timesteps.<sup>39</sup> To remove this bias, it is common to use multiple timesteps to make the linear regression and obtain calculation results for  $\delta t \rightarrow 0$ . This regression is an approximation of the theoretical  $\delta t = 0$  result. The present study considers both linear and quadratic extrapolations.

The software package Gaussian09<sup>40</sup> was used to conduct the MP2 (geometry optimisation), DFT-B3LYP, and CCSD(T) calculations, whereas the CASINO<sup>41</sup> code was used to apply the FNDMC calculations. An electron-nucleus cusp correction scheme<sup>24</sup> for Gaussian orbitals was utilised in the all-electron FNDMC calculation in CASINO. In addition, cc-pCV $x$ Z ( $x = \text{D, T, Q}$ ) basis sets for Si and O as well as the corresponding cc-pV $x$ Z versions for the H atoms during the same calculations were obtained from the online Basis Set Exchange library.<sup>42</sup> In FNDMC for both structures, the number of target population was 11,520, and the number of steps in the imaginary-time evolution was set to 2,000 and 500,000 for equilibrated and accumulated phases, respectively. In addition, we carried out FNDMC calculations with different timesteps of 0.01, 0.005, and 0.001 to remove the short-time bias (see SI for more details).

## RESULTS and DISCUSSION

### Geometry and ZPE contribution

Several studies have been conducted on the geometry of the disiloxane molecule, although most *ab initio* methods tested did not manage to replicate the available experimental results. Rather than the Si-O bond length, the Si-O-Si bond angle and linearisation barrier have been found to be greatly dependent on the choice of basis set used to represent the wavefunction.<sup>8</sup> This study focuses on the linearisation barrier of disiloxane, taking the same optimised geometries for all calculations, partly owing to the notorious difficulty in optimising the geometries in FNDMC.

The computational and experimental linearisation barriers of disiloxane,  $\Delta E_{\text{barrier}}$ , defined in Eq. (1) are listed in Table 2 and plotted in Figure 2 as a visual guide. It has been commonly observed experimentally that the non-linear (bent) structure

**Table 2: Linearisation barrier values obtained from theoretical calculations and experiments. Its ZPE correction and ZPE-corrected Raman value are also given. Computational values ( $\Delta\epsilon_0$ ) are to be compared with a ZPE-corrected experimental value ( $\Delta\epsilon_1 - \Delta ZPE$ ); see the text for the definition of notation, sign, etc. .**

Basis set	$\Delta\epsilon_0$ [kcal/mol]		
	DFT-B3LYP	CCSD(T)	FNDMC
cc-pVDZ	0.80	1.44	0.40 $\pm$ 0.15
cc-pCVDZ	0.76	1.42	0.54 $\pm$ 0.12
cc-pVTZ	0.18	0.46	0.47 $\pm$ 0.14
cc-pCVTZ	-0.01	0.32	0.31 $\pm$ 0.11
cc-pVQZ	0.18	0.44	0.26 $\pm$ 0.10
cc-pCVQZ	0.06	0.35	0.36 $\pm$ 0.10
	$\Delta\epsilon_1$ [kcal/mol]		$\Delta\epsilon_1 - \Delta ZPE$ [kcal/mol]
Far IR spectrum <sup>25</sup>	IR-Raman (solid) <sup>2</sup>	Raman <sup>3</sup>	ZPE-corrected Raman ( $\Delta ZPE$ ) <sup>6</sup>
1.1-1.4	0.32	0.3	0.36 (-0.06)

of disiloxane is energetically more favourable than a linear structure, which translates to a positive linearisation barrier. All three experimental results seem to agree on this point, and<sup>25</sup> in particular reports a higher linearisation barrier (at 1.1 to 1.4 kcal/mol) than the other two results,<sup>2,3</sup> which report a barrier of approximately 0.3 kcal/mol. Both of these measurements are more recent than the first and achieve good consilience with the DFT predictions from the highest quality basis sets.<sup>8</sup> Therefore, it is reasonable to infer that a linearisation barrier of approximately 0.3 kcal/mol is a reliable value for disiloxane.

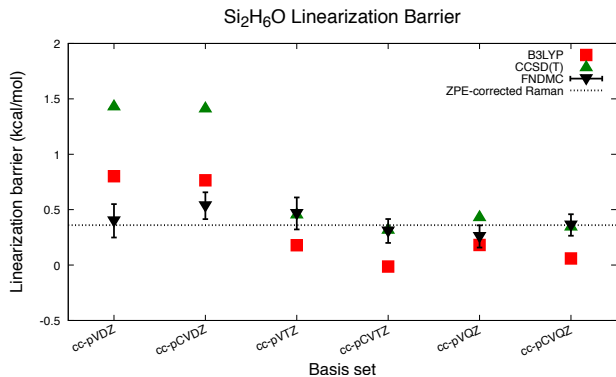


**Figure 2: Linearisation barrier of disiloxane calculated in this work.**

It needs to be stressed, however, that the experimentally measured linearisation barrier may not be comparable to the ground state values calculated from the first principles. The ground state energy

obtained through *ab initio* calculations are physically unobtainable experimentally because of the ZPE, i.e. the difference between the ground state and the lowest energy vibrational state. Even at absolute zero temperature, the lowest energy level achievable is a vibrational state  $\epsilon_1$  instead of the electronic ground state  $\epsilon_0$ :

$$\epsilon_1 = \epsilon_0 + ZPE \quad (2)$$

Consequently, any energetic barriers measured in the experiments is at best the difference between the lowest vibrational states  $\Delta\epsilon_1$ , whereas energetic barriers calculated through *ab initio* methods are from the electronic ground states  $\Delta\epsilon_0$ . Therefore, a comparison between energetic barriers obtained from the theoretical calculations and experimental measurements must also account for the difference in ZPE. The energetic barrier of a transition from quantum state A to state B is calculated as follows:

$$\begin{aligned} \epsilon_1^B - \epsilon_1^A &= (\epsilon_0^B + ZPE^B) - (\epsilon_0^A + ZPE^A) \\ \epsilon_1^B - \epsilon_1^A &= (\epsilon_0^B - \epsilon_0^A) + (ZPE^B - ZPE^A) \\ \Delta\epsilon_1 &= \Delta\epsilon_0 + \Delta ZPE \\ \Delta\epsilon_0 &= \Delta\epsilon_1 - \Delta ZPE \end{aligned} \quad (3)$$

The difference in ZPE  $\Delta ZPE$  between the initial and final states  $A \rightarrow B$  is usually considered insignificant. However, barrier height discrepancies on the order of 0.1 kcal/mol might well be caused

by this term.

The preceding theoretical study by Koput<sup>6</sup> estimates a  $\Delta ZPE$  value of  $-20 \text{ cm}^{-1} \approx -0.06 \text{ kcal/mol}$ , which in line with Equation 3 should result in a higher ground state linearisation barrier than the experimentally measured result. Therefore, this study treats the ground state linearisation barrier of  $0.36 \text{ kcal/mol}$  as a reasonably accurate “exact” linearisation barrier for a point of comparison with *ab initio* calculations. This value is referred to as “ZPE-corrected Raman” in Table 2 and based on a dotted line in the figures herein, as a point of comparison. ZPE correction has not been considered in *ab initio* comparisons or based on experimental results, which have cited  $0.3 \text{ kcal/mol}$  as the point of comparison.<sup>8</sup>

## DFT-B3LYP results

Both the cc-pVxZ and cc-pCVxZ basis sets show positive linearisation barriers (except for cc-pCVTZ), energetically favouring the non-linear over the linear conformer of disiloxane. The simplest basis set, i.e. the double zeta cc-pVDZ basis set, results in the highest barrier of all ( $0.80 \text{ kcal/mol}$ ), in certain agreement with the far infrared absorption spectra of gaseous disiloxane.<sup>25</sup> The core-valence correlated counterpart, i.e. the cc-pCVDZ basis set, also produces a high linearisation barrier of  $0.78 \text{ kcal/mol}$ . Triple zeta basis sets (cc-pVTZ and cc-pCVTZ) show a significant reduction in the barrier height, eventually converging to the quadruple zeta set results. These results reinforce the conclusions drawn in preceding studies<sup>5–8,11</sup> that the basis sets at the double zeta level are insufficient to properly describe the disiloxane molecular properties, and that the triple zeta level is the minimally reliable level for the description of the atomic orbitals. The trends of the linearisation barrier, meanwhile, is nearly identical for both standard and core-correlated variants (Figure 4), with higher quality sets producing good agreement with two of the three available experimental results.<sup>2,3</sup>

The results for DFT-B3LYP in this study, particularly the converged results for the quadruple zeta basis sets cc-pVQZ and cc-pCVQZ, seem to indicate that previous agreement between the B3LYP

results and experimental data<sup>8</sup> is due to coincidence instead of convergence toward the complete basis set limit. Indeed, for the largest basis sets used in this study, the linearisation barrier calculated by B3LYP is at best approximately  $0.1 \text{ kcal/mol}$  smaller than the ZPE-corrected measurement. It does not seem that the B3LYP exchange-correlation functional provides adequate accounting of the electron correlation for properly describing a disiloxane molecule.

## CCSD(T) results

CCSD(T) calculations were conducted with the same geometries and basis sets as the B3LYP calculations. The results of these calculations are shown in Table 2. The trends of the linearisation barrier agree almost perfectly with B3LYP calculations, with a universal shift in the energetic favourability toward the non-linear conformer denoted by the larger linearisation barriers. CCSD(T) calculations seem to converge to values closer to the ZPE-corrected Raman linearisation barrier of  $0.36 \text{ kcal/mol}$ . The cc-pVxZ basis sets converge to a linearisation barrier of approximately  $0.44 \text{ kcal/mol}$ , whereas the core-valence correlated set cc-pCVxZ converges to a barrier height of approximately  $0.35 \text{ kcal/mol}$ , in excellent agreement with the benchmark value. We also achieved good agreement with another CCSD(T) calculation in an earlier study<sup>8</sup> reporting a linearisation barrier of  $0.48 \text{ kcal/mol}$  using the cc-pVTZ basis set. These results show that accounting for the electron correlation is indeed necessary to properly model the Si-O-Si bond in disiloxane, and supports the conclusion of earlier studies citing cc-pVTZ and CCSD(T) as the minimum reliable level of description for the disiloxane molecule.<sup>7,8</sup>

## FNDMC results

The linearisation barrier calculated by FNDMC is also shown in Table 2 and Figure 2. As with CCSD(T), the linearisation barrier values from FNDMC converge to a value close to the ZPE-corrected Raman benchmark adopted in this study of  $0.36 \text{ kcal/mol}$  for the largest basis sets. Also observed is the independence of the linearisation bar-

rier calculated from the basis set used to form the initial trial wavefunction using DFT-B3LYP relative to the other two calculation methods. The influence of the different basis sets on the end result of the FNDMC calculations directly translates into how they affect the trial wavefunction nodal surfaces. The amplitudes of the trial wavefunction, meanwhile, do not affect the end result at ( $\tau \rightarrow \infty$ ), which, in turn, limits the dependence of the end result on the basis sets used to form the trial wavefunction.

The quality of the trial wavefunction nodal surface (how close it resembles the true ground-state wavefunction nodal surface) is reflected in the total energy values of the FNDMC calculation (the fixed-node variational principle).<sup>13</sup> Therefore, the expected values of the total energy in the all-electron FNDMC calculations (such as those conducted in this study) are good indicators of the quality of the trial wavefunction nodal surfaces, because all-electron FNDMC calculations retain the variational principle with respect to the total energy of the ground-state. These absolute values are shown in Table 3, sorted in accord with the quality of the nodal surface (from low quality, high total energy, to high quality, low total energy), and displayed in Figure 3. It can be observed that the cc-pCVTZ produces a nodal surface of slightly better quality than cc-pVQZ, indicating that the electron correlation between the core and valence electrons can be a significant factor for improvement beyond the triple zeta level of atomic orbital description.

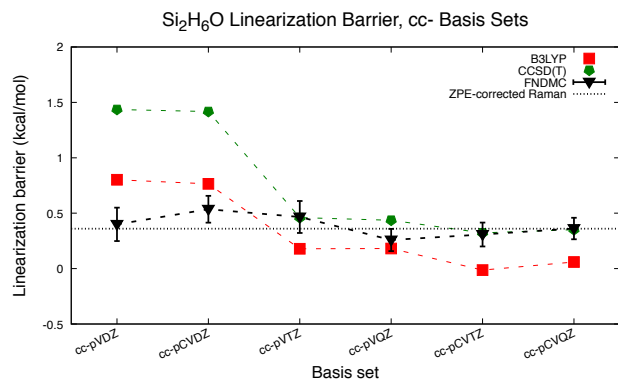


Figure 3: Linearisation barrier of disiloxane calculated using cc- basis sets, sorted based on the quality of the nodal surface. Dashed lines serve to better illustrate the trends present in the data.

## Effects of basis sets

Disiloxane linearisation barrier dependence on the basis set was observed for all cases. In agreement with previous studies,<sup>8</sup> this dependence is more significant than the methodologies used in the *ab initio* calculations, particularly considering the double zeta-level basis sets cc-pVDZ and cc-pCVDZ. Triple zeta basis sets seem to offer the minimum level of description to reliably predict the linearisation barrier, whereas quadruple zeta basis sets result in an extremely good prediction, especially for the CCSD(T) and FNDMC calculations. Figure 2 clearly shows very similar trends for each calculation method with a substantial dependence on the basis set indicated, particularly towards the smaller sets. Convergence of the disiloxane linearisation barrier is generally observed for all three calculation methods, albeit not necessarily converging to the same value.

Previous theoretical studies suggest that this converging trend is attributed to the increasing addition of polarisation functions<sup>8</sup> within the basis sets used. Adding polarisation functions serves to better reproduce dynamical correlations in the system. This is in line with previous theoretical works with semi-empirical methods implying that calculations without electron correlation favour the linear structure, thereby resulting in negative values of linearisation barrier. This is also reflected in preceding geometry optimisation calculations without polarisation functions, resulting in Si-O-Si angles close to 170°. <sup>4,5</sup> Therefore, it is expected that both cc-pVxZ and cc-pCVxZ basis sets should converge to a reliable predicted linearisation barrier value because polarisation functions are systematically included with an increasing description of the atomic orbitals.

From Figure 4, a comparison can be observed between the correlation consistent cc-pVxZ basis sets and its core-valence correlated counterpart cc-pCVxZ. The B3LYP and CCSD(T) linearisation barrier trends closely follow one another, with CCSD(T) cc-pCVxZ in particular converging to a nearly identical value as that of the ZPE-corrected Raman. Meanwhile, the FNDMC results show a slight difference in the trends between the two families when observing the respective expecta-

**Table 3: Total energies from FNDMC calculations, sorted from highest to lowest.**

Basis set	$E_{\text{total}}$ [Hartree]	
	Delinear	Linear
cc-pVDZ	-657.7994(2)	-657.7988(2)
cc-pCVDZ	-657.8062(1)	-657.8053(1)
cc-pVTZ	-657.8270(2)	-657.8263(2)
cc-pVQZ	-657.8366(1)	-657.8362(1)
cc-pCVTZ	-657.8376(1)	-657.8371(1)
cc-pCVQZ	-657.8437(1)	-657.8431(1)

tion values of the linearisation barriers. It should be noted, however, that the stochastic nature of FNDMC diminishes the significance of the energy trends (which need to be considered probabilistically).

Figure 3 shows that FNDMC is overall less dependent on the basis set used compared to both B3LYP and CCSD(T). Although previous studies have recommended treating disiloxane with the cc-pVTZ basis set at a minimum, cc-pVDZ is shown to generate a sufficiently high quality nodal surface for use in DMC calculations, giving a linearisation barrier in good agreement with the experimental values. Even for the smallest basis sets tested in this study, FNDMC shows relatively more accurate values of the linearisation barrier, and therefore less dependence on the basis set used to form the trial wavefunction per the initial expectations.

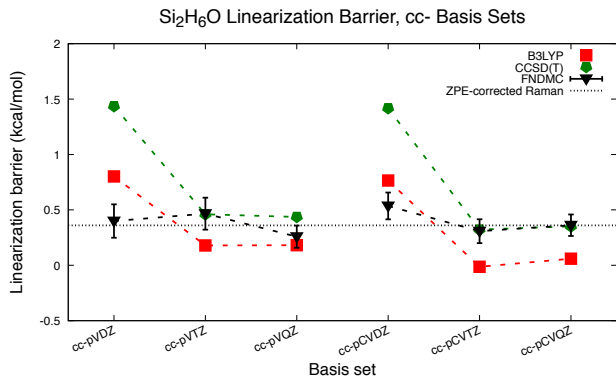


Figure 4: Linearisation barrier of disiloxane calculated using cc-basis sets, separated into standard and core-valence-correlated versions (left and right). Dashed lines serve to better illustrate the trends present in the data.

## Effects of methodologies

In line with previous studies, we find the dependence on the methods weaker than that on the basis sets. With increasing levels of basis sets, DFT-B3LYP and CCSD(T) values of the linearisation barriers converge to approximately 0.1 and 0.3-0.4 kcal/mol, respectively. This slight difference is in accord with the variance in experimental measurements<sup>2,3,25</sup> and is clearly less significant than the variance as a result of the basis sets.

Previous expectations on the trend in methodologies are derived from previous studies,<sup>4,43</sup> particularly the study by Koput in 1990,<sup>4</sup> in which the inclusion of the electron correlation proved vital to predicting the energetic favourability of the non-linear structure of disiloxane because the SCF calculation produced a near-linear structure of disiloxane. This and other studies<sup>43</sup> gave rise to the general expectation that the inclusion of an electron correlation is important to properly model the structure of disiloxane. As previously mentioned, it can be observed that the B3LYP exchange-correlation functional is insufficient to properly recover the electron correlation and thereby predict the disiloxane linearisation barrier. Meanwhile, CCSD(T) and FNDMC calculations both converge towards the ZPE-corrected Raman value, indicating a proper accounting of the dynamical correlation.

FNDMC has the added advantage of being able to reliably predict the energetics of disiloxane with smaller basis sets. With better scalability for application in high performance computing (HPC) systems and the availability of pseudopotentials, FNDMC is a promising alternative method to CCSD(T) for describing the Si-O-Si bonds, par-



ticularly for larger systems.

## CONCLUSION

The Si<sub>2</sub>H<sub>6</sub>O linearisation barrier was calculated using three separate *ab initio* methods, DFT-B3LYP, CCSD(T), and FNDMC, with six different basis set choices in line with expectations derived from previous theoretical studies on disiloxane. Similar with previous studies, we observed that the systematic inclusion of polarisation functions, along with an increasing level of description for atomic orbitals, eventually result in a reliable prediction of the disiloxane linearisation barrier. All calculation methods eventually produced converged values with increasing level of basis sets for the linearisation barrier, with 0.1 kcal/mol for DFT-B3LYP and 0.3-0.4 kcal/mol for CCSD(T), respectively, in line with previous theoretical studies,<sup>8</sup> and similar expectation values of the barrier for FNDMC calculations. The agreement between the experimental measurements and the DFT-B3LYP results at 0.3 kcal/mol are shown to be likely accidental. ZPE-corrected experimental measurements are in good agreement with the CCSD(T) and FNDMC results, with the ground state linearisation barrier taken at 0.36 kcal/mol. FNDMC is shown to be least dependent on the choice of basis set among the three calculation methods applied, in line with initial expectations owing to the nature of FNDMC.

## ACKNOWLEDGEMENTS

The computations in this study were conducted using the facilities of Research Center for Advanced Computing Infrastructure at JAIST. R.M. would like to extend his appreciation for the financial support from MEXT-KAKENHI (19H04692 and 16KK0097), FLAGSHIP2020 (project nos. hp190169 and hp190167 at K-computer), the Air Force Office of Scientific Research (AFOSR-AOARD/FA2386-17-1-4049;FA2386-19-1-4015), and JSPS Bilateral Joint Projects (with India DST). K.H. would like to thank the HPCI System Research Project (Project ID: hp190169) and MEXT-KAKENHI (JP16H06439, JP17K17762,

JP19K05029, and JP19H05169) for the financial support.

## References

- (1) Luke, B. T. An *ab initio* investigation of the lowest potential energy surface of disiloxane. *J. Phys. Chem.* **1993**, *97*, 7505–7510.
- (2) Durig, J. R.; Flanagan, M. J.; Kalasinsky, V. F. The determination of the potential function governing the low frequency bending mode of disiloxane. *J. Chem. Phys.* **1977**, *66*, 2775.
- (3) Koput, J. The large-amplitude motions in quasi-symmetric top molecules with internal C<sub>3v</sub> rotors: Interpretation of the low frequency Raman spectrum of disiloxane. *J. Mol. Spec.* **1983**, *99*, 116–132.
- (4) Koput, J. *Ab initio* study of the molecular structure and potential energy surface of disiloxane. *J. Chem. Phys.* **1990**, *148*, 299–308.
- (5) Csonka, G. I.; Réffy, J. Density functional study of the equilibrium geometry and Si-O-Si potential energy curve of disiloxane. *Chem. Phys. Lett.* **1994**, *229*, 191–197.
- (6) Koput, J. An *ab Initio* Study on the Potential Energy Surface of Large-Amplitude Motions for Disiloxane. *J. Phys. Chem.* **1995**, *99*, 15874–15880.
- (7) Carteret, C.; Labrosse, A.; Assfeld, X. An *ab initio* and DFT study of structure and vibrational spectra of disiloxane H<sub>3</sub>SiOSiH<sub>3</sub> conformers: Comparison to experimental data. *Spectrochimica Acta Part A* **2007**, *67*, 1421–1429.
- (8) Derzi, A. R. A.; Gregušová, A.; Runge, K.; Bartlett, R. J. Structure and properties of disiloxane: an *ab initio* and post-Hartree-Fock study. *Int. J. Quantum Chem.* **2008**, *108*, 2088–2096.
- (9) Noritake, F.; Kawamura, K. The nature of Si-O-Si bonding via Molecular Orbital calculations. *J. Comput. Chem. Jpn.* **2015**, *14*, 124–130.

- (10) Noritake, F. Revisiting the Nature of Si-O-Si Bridging. *J. Comput. Chem. Jpn.-Int. Ed.* **2019**, *5*, 2018–0016.
- (11) Nicholas, J. B.; Feyereisen, M. An evaluation of correlation-consistent basis sets in calculating the structure and energetics of  $(\text{H}_3\text{Si})_2\text{O}$ ,  $\text{H}_3\text{SiOH}$ , and  $\text{H}_3\text{SiO}^-$ . *J. Chem. Phys.* **1995**, *103*, 8031.
- (12) Yuan, X.; Cormack, A. N. Si-O-Si bond angle and torsion angle distribution in vitreous silica and sodium silicate glasses. *J. Non-Cryst. Solids* **2003**, *319*, 31–43.
- (13) Foulkes, W. M. C.; Mitas, L.; Needs, R. J.; Rajagopal, G. Quantum Monte Carlo simulation of solids. *Rev. Mod. Phys.* **2001**, *73*, 33.
- (14) Hongo, K.; Watson, M. A.; Sánchez-Carrera, R. S.; Iitaka, T.; Aspuru-Guzik, A. Failure of Conventional Density Functionals for the Prediction of Molecular Crystal Polymorphism: A Quantum Monte Carlo Study. *J. Phys. Chem. Lett.* **2010**, *1*, 1789–1794.
- (15) Watson, M. A.; Hongo, K.; Iitaka, T.; Aspuru-Guzik, A. *Advances in Quantum Monte Carlo*; Chapter 10, pp 101–117.
- (16) Hongo, K.; Cuong, N. T.; Maezono, R. The Importance of Electron Correlation on Stacking Interaction of Adenine-Thymine Base-Pair Step in B-DNA: A Quantum Monte Carlo Study. *J. Chem. Theory Comput.* **2013**, *9*, 1081–1086.
- (17) Hongo, K.; Iitaka, T.; Watson, M.; Aspuru-Guzik, A.; Maezono, R. Diffusion Monte Carlo study of Para-Diiodobenzene Polymorphism Revisited. *J. Chem. Theory Comput.* **2015**, *11*, 907–917.
- (18) Koseki, J.; Maezono, R.; Tachikawa, M.; Towler, M. D.; Needs, R. J. Quantum Monte Carlo study of porphyrin transition metal complexes. *J. Chem. Phys.* **2008**, *129*, 085103:1–5.
- (19) Hongo, K.; Maezono, R. A computational scheme to evaluate Hamaker constants of molecules with practical size and anisotropy. *J. Chem. Theory Comput.* **2017**, *13*, 5217–5230.
- (20) Takagishi, H.; Matsuda, T.; Shimoda, T.; Maezono, R.; Hongo, K. Method for the Calculation of the Hamaker constants of Organic Materials by the Lifshitz Macroscopic Approach With DFT. *J. Phys. Chem.* **2019**, *A 123*, 8726–8733.
- (21) Ichibha, T.; Hou, Z.; Hongo, K.; Maezono, R. New Insight into the Ground State of FePc: A Diffusion Monte Carlo Study. *Sci. Rep.* **2017**, *7*, 2011.
- (22) Nakano, K.; Maezono, R.; Sorella, S. All-electron quantum Monte Carlo with Jastrow single determinant Ansatz: application to the sodium dimer. *J. Chem. Theory Comput.* **2019**, *15*, 4044–4055.
- (23) Maezono, R. Optimization of Many-body Wave function. *J. Comput. Theor. Nanosci.* **2009**, *6*, 2474–2482.
- (24) Ma, A.; Towler, M. D.; Drummond, N. D.; Needs, R. J. Scheme for adding electron-nucleus cusps to Gaussian orbitals. *J. Chem. Phys.* **2005**, *122*, 224322.
- (25) Aronson, J. R.; Lord, R. C.; Robinson, D. W. Far Infrared Spectrum and Structure of Disiloxane. *J. Chem. Phys.* **1960**, *33*, 1004.
- (26) Jr., T. H. D. Gaussian basis sets for use in correlated molecular calculations. I. The atoms boron through neon and hydrogen. *J. Chem. Phys.* **1989**, *90*, 1007.
- (27) Kendall, R. A.; Jr., T. H. D. Electron affinities of the first-row atoms revisited. Systematic basis sets and wave functions. *J. Chem. Phys.* **1992**, *96*, 6796.
- (28) Woon, D. E.; Jr., T. H. D. Gaussian basis sets for use in correlated molecular calculations. III. The atoms aluminum through argon. *J. Chem. Phys.* **1993**, *98*, 1358.

- (29) Peterson, K. A.; Dunning, T. H. Accurate correlation consistent basis sets for molecular core-valence correlation effects: The second row atoms Al-Ar, and the first row atoms B-Ne revisited. *J. Chem. Phys.* **2002**, *117*, 10548.
- (30) Almenningen, A.; Bastiansen, O.; Ewing, V.; Hedberg, K.; Traetteberg, M. The molecular structure of disiloxane (SiH<sub>3</sub>)<sub>2</sub>O. *Acta Chem. Scand* **1963**, *17*.
- (31) Becke, A. D. A new mixing of Hartree-Fock and local density-functional theories. *J. Chem. Phys.* **1993**, *98*, 1372.
- (32) Monkhorst, H. J. Calculation of properties with the coupled-cluster method. *International Journal of Quantum Chemistry* **1977**, *12*, 421–432.
- (33) Woon, D. E.; Jr., T. H. D. Gaussian basis sets for use in correlated molecular calculations. V. Core-valence basis sets for boron through neon. *J. Chem. Phys.* **1995**, *103*, 4572.
- (34) Jastrow, R. Many-Body Problem with Strong Forces. *Phys. Rev.* **1955**, *98*, 1479–1484.
- (35) Drummond, N. D.; Towler, M. D.; Needs, R. J. Jastrow correlation factor for atoms, molecules, and solids. *Phys. Rev. B* **2004**, *70*, 235119.
- (36) Drummond, N. D.; Needs, R. J. Variance-minimization scheme for optimizing Jastrow factors. *Phys. Rev. B* **2005**, *72*, 085124.
- (37) Kato, T. On the Eigenfunctions of Many-Particle Systems in Quantum mechanics. *Commun. Pure Appl. Math.* **1957**, *10*, 151–177.
- (38) Reynolds, P. J.; Ceperley, D. M. Fixed-node quantum Monte Carlo for molecules. *J. Chem. Phys.* **1982**, *77*, 5593.
- (39) Umrigar, C. J.; Nightingale, M. P.; Runge, K. J. A diffusion Monte Carlo algorithm with very small time-step errors. *J. Chem. Phys.* **1993**, *99*, 2865.
- (40) Frisch, M. J.; Trucks, G. W.; Schlegel, H. B.; Scuseria, G. E.; Robb, M. A.; Cheeseman, J. R.; Scalmani, G.; Barone, V.; Mennucci, B.; Petersson, G. A. et al. Gaussian 09. Gaussian Inc. Wallingford CT 2009.
- (41) Needs, R. J.; Towler, M. D.; Drummond, N. D.; Ríos, P. L. Continuum variational and diffusion quantum Monte Carlo calculations. *J. Phys.: Condensed Matter* **2010**, *22*, 023201.
- (42) Pritchard, B. P.; Altarawy, D.; Didier, B.; Gibson, T. D.; Windus, T. L. A New Basis Set Exchange: An Open, Up-to-date Resource for the Molecular Sciences Community. *J. Chem. Inf. Model.* **2019**, *59*, 4814.
- (43) Shambayati, S.; Schreiber, S. L.; Blake, J. F.; Wierschke, S. G.; Jorgensen, W. L. Structure and basicity of silyl ethers: a crystallographic and *ab initio* inquiry into the nature of silicon-oxygen interactions. *J. Am. Chem. Soc.* **1990**, *112*, 697–703.